symmetry

MDPI

Article

Einstein–Gauss–Bonnet Gravity with Nonlinear Electrodynamics: Entropy, Energy Emission, Quasinormal Modes and Deflection Angle

Sergey Il'ich Kruglov [1,2]

[1] Department of Physics, University of Toronto, 60 St. Georges St., Toronto, ON M5S 1A7, Canada; serguei.krouglov@utoronto.ca
[2] Department of Chemical and Physical Sciences, University of Toronto, 3359 Mississauga Road North, Mississauga, ON L5L 1C6, Canada

Abstract: The logarithmic correction to Bekenshtein–Hawking entropy in the framework of 4D Einstein–Gauss–Bonnet gravity coupled with nonlinear electrodynamics is obtained. We explore the black hole solution with the spherically symmetric metric. The logarithmic term in the entropy has a structure similar to the entropy correction in the semi-classical Einstein equations. The energy emission rate of black holes and energy conditions are studied. The quasinormal modes of a test scalar field are investigated. The gravitational lensing of light around BHs was studied. We calculated the deflection angle for some model parameters.

Keywords: Einstein–Gauss–Bonnet gravity; nonlinear electrodynamics; entropy; energy emission; quasinormal modes; deflection angle

Citation: Kruglov, S.I. Einstein–Gauss–Bonnet Gravity with Nonlinear Electrodynamics: Entropy, Energy Emission, Quasinormal Modes and Deflection Angle. *Symmetry* **2021**, *13*, 944. https://doi.org/10.3390/sym13060944

Academic Editor: Alexander Shalyt-Margolin

Received: 17 April 2021
Accepted: 19 May 2021
Published: 26 May 2021

1. Introduction

A valuable fundamental quantum theory of gravity should be renormalizable and unitary but general relativity (GR) is perturbatively nonrenormalizable, but unitary. The renormalizaton of the theory requires higher derivatives in the action and the presence of quadratic terms in curvature can give a renormalizeable theory of quantum gravity. Therefore, a modification of Einstein GR by including higher order curvature terms in action is of interest. It was shown in [1] that quantum corrections in quadratic gravity lead to unstable resonance which does not appear in the asymptotic spectrum. This proves that such theories also are unitary and stable to all orders. The inclusion of terms with four derivatives in the action makes the theory renormalizable, but leads to the presence of ghosts making the perturbative unitarity of the theory questionable. The authors of [2] showed that such spin-2 ghosts do not indicate a violation of unitarity. Higher-derivative corrections in string theory were discussed in [3]. Other applications of models, with higher-order derivatives, in astrophysics and cosmology, were studied in [4].

Another way to take into account higher order curvature terms is to add the Gauss–Bonnet (GB) Lagrangian to Einstein–Hilbert action. Such theory, 4D Einstein–Gauss–Bonnet (4D EGB) gravity in four dimension, recently attracted much attention [5–21]). It was shown by Glavan and Lin [5] that in 4D EGB theory the GB term, which is a topological invariant before regularization, after regularization it is no longer a topological invariant and it contributes to the equation of motion. In [22,23], the authors obtained a solution of the semi-classical Einstein equations with conformal anomaly that also is a solution in the 4D EGB gravity. Recently, the scheme of Glavan and Lin was debated in [24–30]. In particular, it was shown in [27,28] that solutions in the 4D EGB theory differ from GR because they are due to extra infinitely strongly coupled scalar. It is worth noting that the theory of [31–33] gives the solution, in the spherically-symmetric metrics, that is a solution in the framework of rescaling procedure of [5] (see [34]). We explore a BH solution in the 4D EGB gravity

theory coupled to nonlinear electrodynamics (NED) proposed in [35] making use of the theory of [31–33].

Here, we investigate the optical properties of BH by using the solution obtained in 4D EGB gravity coupled to NED. This paper is the continuation of the work [36]. NED considered here possesses the attractive features such as the absence of singularities and simplicity (the solution contains only elementary functions). In addition, at the weak field limit our NED is converted into Maxwell electrodynamics. It worth noting that the solution of well-known Born–Infeld electrodynamics in 4D EGB gravity contains special hypergeometric function [37]. The specific NED can give different astrophysical characteristics: the shadow radius of a charged BH, the BH energy emission rate, and the deflection angle of light from the BH. Therefore it is of interest to test solutions of BHs in 4D EGB gravity coupled to different NED which effect on astrophysical characteristics. Thus, several BH solutions in 4D EGB gravity coupled to NED were studied [11–40]. The quasinormal modes, deflection angle, shadows of BHs and the Hawking radiation were studied in [41–47]. In this paper we analyse the shadow, the energy emission rate, quasinormal modes and the light deflection angle of the magnetically charged BH by using NED proposed in [35].

The paper is organized as follows. In Section 2, we consider the BH spherically symmetric solution in the framework of the 4D EGB gravity. It is shown that at infinity we have the Reissner–Nordström behavior of the charged BH. We obtain the logarithmic correction to Bekenstein–Hawking entropy in Section 3. In Section 4, we study the BH energy emission rate. The energy conditions are investigated in Section 5. It is shown that WEC, DEC and SEC are satisfied. In Section 6, we investigate the BH quasinormal modes and obtain the corresponding frequencies. We study the light defection angle by the BH solution in Section 7. Section 8 is a conclusion.

2. The Model

The EGB gravity action in D-dimensions coupled to NED is

$$I = \int d^D x \sqrt{-g} \left[\frac{1}{16\pi G} (R + \alpha \mathcal{L}_{GB}) + \mathcal{L}_{NED} \right], \tag{1}$$

with α possessing the dimension of (length)^2 and the NED Lagrangian, proposed in [35] is given by

$$\mathcal{L}_{NED} = -\frac{\mathcal{F}}{1 + \sqrt[4]{2\beta\mathcal{F}}}, \tag{2}$$

where the parameter β ($\beta \geq 0$) has the dimension of (length)^4, $\mathcal{F} = (1/4)F_{\mu\nu}F^{\mu\nu} = (B^2 - E^2)/2$, $F_{\mu\nu}$ is the strength tensor and the GB Lagrangian is

$$\mathcal{L}_{GB} = R^{\mu\nu\alpha\beta}R_{\mu\nu\alpha\beta} - 4R^{\mu\nu}R_{\mu\nu} + R^2. \tag{3}$$

The field equation corresponding to action (1) reads

$$R_{\mu\nu} - \frac{1}{2}g_{\mu\nu}R + \alpha H_{\mu\nu} = -8\pi G T_{\mu\nu}, \tag{4}$$

where $T_{\mu\nu}$ is the energy-momentum tensor and

$$H_{\mu\nu} = 2\Big(RR_{\mu\nu} - 2R_{\mu\alpha}R^{\alpha}_{\ \nu} - 2R_{\mu\alpha\nu\beta}R^{\alpha\beta} - R_{\mu\alpha\beta\gamma}R^{\alpha\beta\gamma}_{\ \ \ \nu} \Big) - \frac{1}{2}\mathcal{L}_{GB}g_{\mu\nu}. \tag{5}$$

The spherically symmetric D-dimensional line element is given by

$$ds^2 = -f(r)dt^2 + \frac{dr^2}{f(r)} + r^2 d\Omega^2_{D-2}, \tag{6}$$

where $d\Omega^2_{D-2}$ is the line element of the unit $(D-2)$-dimensional sphere. The Equations (1), (3)–(5) are defined in D dimensions. In the following, we consider rescaling $\alpha \to \alpha/(D-4)$ and the limit $D \to 4$. Following [48] we consider a magnetically charged BH. The magnetic BH represents a magnetic monopole with the magnetic field $B = q_m/r^2$ (q_m is a magnetic charge) and $\mathcal{F} = q_m^2/(2r^4)$. The magnetic energy density is given by

$$\rho = -T_t^{\ t} = -\mathcal{L}_{NED} = \frac{q_m^2}{2r^3(r+\sqrt{q_m}\beta^{1/4})}. \tag{7}$$

The static and spherically symmetric spacetime metric will be used. At the limit $D \to 4$ by exploring the scheme of [5], the tt component of Equation (4) reads

$$r(2\alpha f(r) - r^2 - 2\alpha)f'(r) - (r^2 + \alpha f(r) - 2\alpha)f(r) + r^2 - \alpha = 2r^4 G\rho. \tag{8}$$

The Equation (8) holds for any 4D EGB gravity model with the static and spherically symmetric metric. The general solution to Equation (8) is given by

$$f(r) = 1 + \frac{r^2}{2\alpha}\left(1 \pm \sqrt{1 + \frac{8\alpha G}{r^3}\left(M + \int r^2 \rho dr\right)}\right), \tag{9}$$

where M is the integration constant. For Maxwell electrodynamics the energy density is $\rho = q^2/(2r^4)$ and Equation (9) leads to the metric function obtained in [6]. But at the limit $r \to 0$ that solution leads to the non-physical complex value of the metric function. To have the stable BH [49] we will use the sign minus (the negative branch) before square root in Equation (9). For 4D EGB gravity coupled to NED (2) with the energy density (7), the solution (9) for the negative branch, gives the metric function [36]

$$f(r) = 1 + \frac{r^2}{2\alpha}\left(1 - \sqrt{1 + \frac{8M\alpha G}{r^3} + \frac{4\alpha q_m^{3/2} G}{\beta^{1/4} r^3}\ln\left(\frac{r}{r + \sqrt[4]{\beta q_m^2}}\right)}\right). \tag{10}$$

It should be noted that the limit $\beta \to 0$ for the last term in the square root, by using the L'Hôpital rule, becomes zero. The Weyl tensor for the D-dimensional spatial part of the spherically symmetric D-dimensional line element (6) vanishes. Therefore, the new solution (10) found in the context of [5] is also a new solution for the consistent theory [31–33]. Here we consider pure classical theory and the logarithmic correction in Equation (10) is due to the GB term in the action. With the dimensionless variable $x = r/\sqrt[4]{\beta q_m^2}$, Equation (10) is rewritten as

$$f(x) = 1 + cx^2 - c\sqrt{x^4 + x\left(a + b\ln\left(\frac{x}{x+1}\right)\right)}, \tag{11}$$

where we use the dimensionless parameters

$$a = \frac{8M\alpha G}{\beta^{3/4} q_m^{3/2}}, \quad b = \frac{4\alpha G}{\beta}, \quad c = \frac{\sqrt{\beta} q_m}{2\alpha}. \tag{12}$$

The asymptotic of the metric function $f(r)$ (10), for the negative branch, at $r \gg 1$ is given by

$$f(r) = 1 - \frac{2MG}{r} + \frac{G q_m^2}{r^2} + \mathcal{O}(r^{-3}) \quad r \gg 1. \tag{13}$$

It follows from Equation (13) that M is a magnetic mass of the BH. This equation shows the Reissner–Nordström behavior of the charged BH at large r, and the metric becomes flat at infinity ($r \to \infty$). The asymptotic of the metric function $f(r)$, for the positive branch, does not correspond to the BH with the Reissner–Nordström behavior at infinity. It is worth noting that the condition $x^4 + x(a + b\ln(x/(x+1))) > 0$ should be satisfied to have the real metric function $f(x)$. This requirement gives the restriction on the radius.

The nontrivial solution x_0 to the equation $x^4 + x(a + b\ln(x/(x+1))) = 0$ leads to the limitation $x > x_0$. One can verify that curvature invariants, Ricci and Kretschmann scalars, have singularities at $x = x_0$. Thus, the spacetime developed a spacetime singularity at $x = x_0$.

3. Thermodynamics and BH Entropy

By using the expression for Hawking temperature $T_H(r_+) = f'(r_+)/(4\pi)$, where r_+ is the event horizon radius, $f(r_+) = 0$, and the prime means the derivative with respect to the argument, we obtain [36]

$$T_H(x_+) = \frac{(2cx_+^2 - 1)(1 + x_+) - bc^2 x_+}{8\pi \sqrt[4]{\beta q_m^2} x_+ (1 + x_+)(1 + cx_+^2)}, \tag{14}$$

where $x_+ = r_+/\sqrt[4]{\beta q_m^2}$. The BH gravitational mass, found from equation $f(x_+) = 0$, reads

$$M(x_+) = \frac{\beta^{3/4} q_m^{3/2}}{8\alpha G}\left(\frac{1 + 2cx_+^2}{c^2 x_+} - b\ln\left(\frac{x_+}{x_+ + 1}\right)\right). \tag{15}$$

According to the first law of BH thermodynamics $dM(x_+) = T_H(x_+)dS + \phi dq$ (ϕ is an electromagnetic potential) the entropy S at the constant charge q is given by

$$S = \int \frac{dM(x_+)}{T_H(x_+)} = \int \frac{1}{T_H(x_+)} \frac{\partial M(x_+)}{\partial x_+} dx_+. \tag{16}$$

With the help of Equations (14)–(16) we find the entropy

$$S = \frac{4\pi\alpha}{G}\int \frac{1 + cx_+^2}{x_+} dx_+ = \frac{\pi r_+^2}{G} + \frac{4\pi\alpha}{G}\ln\left(\frac{r_+}{\sqrt[4]{\beta q_m^2}}\right) + C, \tag{17}$$

were C is the integration constant. It is worth noting that there is uncertainty in the choice of C [50]. It is convenient to use the integration constant C in the form

$$C = \frac{2\pi\alpha}{G}\ln\left(\frac{\pi q_m \sqrt{\beta}}{G}\right). \tag{18}$$

With Equations (17) and (18) one obtains the entropy

$$S = S_0 + \frac{2\pi\alpha}{G}\ln(S_0), \tag{19}$$

where $S_0 = \pi r_+^2/G$ is the Bekenstein–Hawking entropy. In accordance with Equation (19) the entropy includes the Bekenstein–Hawking entropy and the logarithmic correction. The attractive feature of entropy (19) is that it does not depend on the NED parameter β. Thus, there is not singularity of the entropy in the case $\beta = 0$. It should be noted that the entropy, similar to Equation (19) with the logarithmic term, appears in GR containing a conformal anomaly, and also in loop quantum gravity and in the theory of strings [22,23,50,51]. When $\alpha \to 0$ the entropy (19) becomes the Bekenstein–Hawking entropy. For the big event horizon radiuses the leading term of the entropy is the area law and for small x_+ the logarithmic correction is dominant. It has to be noted that at some parameters α, β, q_m and r_+ the entropy vanishes. The entropy (17) (with $C = 0$) is zero when the event horizon radius obeys the equation $r_+^4 \exp(r_+^2/\alpha) = \beta q_m^2$ which is $r_0 = \sqrt{2\alpha W_0(\sqrt{\beta} q_m/(2\alpha))}$, where $W_0(x)$ is the Lambert function. The similar solution r_0 to Equation (19) for $S = 0$ is given by $r_0 = \sqrt{2\alpha W_0(G/(2\pi\alpha))}$. At $r_+ < r_0$ the entropy is negative and such a situation takes place in the model of [52].

4. The Energy Emission Rate

The shadow of BHs is linked with the high energy absorption cross section σ seen for the observer at infinity [53–55] (see also [56]). The absorption cross-section, at very high energies, oscillates about an approximate value of the photon sphere $\sigma \approx \pi r_s^2$, where x_s defines the BH shadow radius $r_s = x_s \sqrt[4]{\beta q_m^2}$ (the impact parameter). The shadow radius can be expressed through the radius of the photon sphere r_p by the relation $r_s = r_p/f(r_p)$ for a distant observer, and r_p is the solution of the equation $f'(r_p)r_p - 2f(r_p) = 0$ [36]. The energy emission rate in the high energy is given by

$$\frac{d^2E(\omega)}{dtd\omega} = \frac{2\pi^3\omega^3 r_s^2}{\exp(\omega/T_H(r_+)) - 1}. \tag{20}$$

Here, ω is the emission frequency and T_H is the Hawking temperature. With the help of the dimensionless variables $x = r/\sqrt[4]{\beta q_m^2}$, $\bar{T}_H(x_+) = \sqrt[4]{\beta q_m^2}T_H(x_+)$, and Equation (20), we obtain

$$\beta^{1/4}\sqrt{q_m}\frac{d^2E(\omega)}{dtd\omega} = \frac{2\pi^3\varpi^3 x_s^2}{\exp(\varpi/\bar{T}_H(x_+)) - 1}, \tag{21}$$

and the Hawking temperature is given by Equation (14) and $\varpi = \beta^{1/4}\sqrt{q_m}\omega$. For some parameters b at $a = 5$, $c = 1$ we obtain the event horizon radius, the photon sphere radius and the shadow radius (expressed via the dimensionless variables) presented in Table 1 (see also [36]). It is worth noting that the parameters a, b and c are connected with M, α, β and q_m by Equation (12). Because there are many parameters in the model, we use in Table 1 some set as an example.

Table 1. The event horizon, photon sphere and shadow dimensionless radii for a = 5, c = 1.

b	0.5	0.9	1.5	1.7	1.8	2	2.2	2.3	2.4	2.5	2.6
x_+	2.18	2.08	1.93	1.87	1.84	1.77	1.69	1.65	1.61	1.56	1.51
x_p	3.42	3.31	3.12	3.05	3.01	2.94	2.86	2.82	2.77	2.73	2.68
x_s	6.16	6.02	5.78	5.70	5.65	5.56	5.47	5.42	5.37	5.32	5.26

Making use of the data given in Table 1 we depicted the plot of the emission rate in Figure 1 for $c = 1$, $a = 5$ and $b = 1.5, 2, 2.5$. According to Figure 1 there is a peak of the energy emission rate for the BH depending on model parameters. When the parameter b increases, the maximum of the peak decreases and possesses the low frequency. Thus, the BH has a bigger lifetime at a bigger parameter b. One can investigate the dependence of the energy emission rate on parameters α, β, q_m and M, putting some numerical values for them.

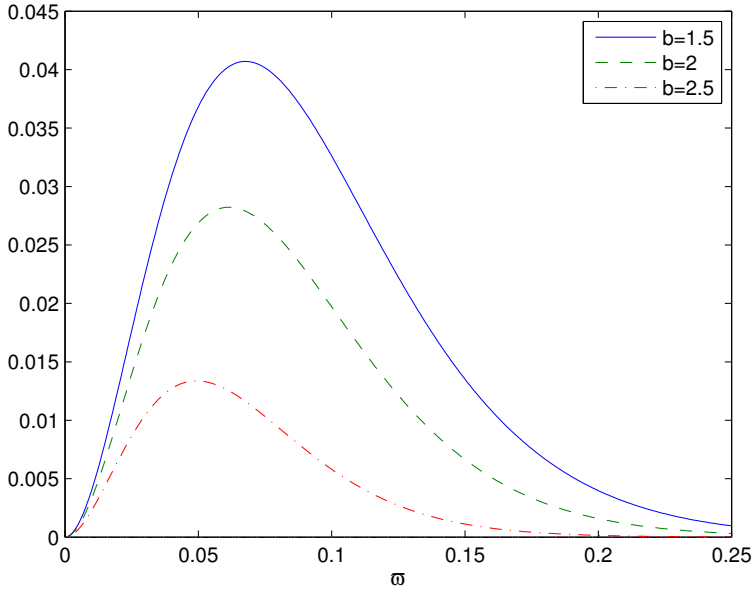

Figure 1. The plot of the function $\beta^{1/4}\sqrt{q_m}\frac{d^2E(\omega)}{dtd\omega}$ vs. ϖ for $b = 1.5, 2, 2.5$, $a = 5$, $c = 1$.

5. The Energy Conditions

The symmetrical energy-momentum tensor with the spherically symmetry leads to ${T_t}^t = {T_r}^r$ and the radial pressure is given by $p_r = -{T_r}^r = -\rho$. The tangential pressure is defined as $p_\perp = -{T_\vartheta}^\vartheta = -{T_\phi}^\phi$ so that [57]

$$p_\perp = -\rho - \frac{r}{2}\rho'(r), \tag{22}$$

where the prime means the derivative with respect to the argument. The weak energy condition (WEC) is satisfied when $\rho \geq 0$ and $\rho + p_k \geq 0$ (k = 1,2,3) [58]. This guarantees that the energy density is non-negative as measured by any local observer. In accordance with Equation (7) $\rho \geq 0$. Making use of Equation (7) one finds

$$\rho'(r) = -\frac{q_m^2(4r + 3\beta^{1/4}\sqrt{q_m})}{2r^4(r + \beta^{1/4}\sqrt{q_m})^2} \leq 0. \tag{23}$$

As a result, we have $\rho \geq 0$, $\rho + p_r = 0$, $\rho + p_\perp \geq 0$ and WEC holds. The dominant energy condition (DEC) takes place when [58] $\rho \geq 0$, $\rho + p_k \geq 0$, $\rho - p_k \geq 0$. These conditions include WEC and we have to verify the condition $\rho - p_\perp \geq 0$. From Equations (7), (22) and (23) we obtain

$$\rho - p_\perp = \frac{q_m^{5/2}\beta^{1/4}}{4r^3(r + \sqrt{q_m}\beta^{1/4})^2} \geq 0. \tag{24}$$

Thus, DEC is satisfied. As a result, the sound speed cannot exceed the speed of light. The strong energy condition (SEC) requires the condition $\rho + \sum_{k=1}^{3} p_k \geq 0$ [58]. With the help of Equations (7), (22) and (23) we obtain

$$\rho + \sum_{k=1}^{3} p_k = 2p_\perp = \frac{q_m^2(2r + \sqrt{q_m}\beta^{1/4})}{2r^3(r + \sqrt{q_m}\beta^{1/4})^2} \geq 0, \tag{25}$$

and SEC is satisfied.

6. Quasinormal Modes

Quasinormal modes (QNMs) are characterised by complex frequencies ω which give an information about the stability of BHs under small perturbations and they do not depend on the initial conditions. The outgoing boundary condition is imposed at infinity

and the ingoing boundary condition at the event horizon. If Im $\omega > 0$ the mode is unstable, otherwise it is stable. It was shown that Re ω in the eikonal limit is linked with the radius of the BH shadow [59,60]. In addition, the real and imaginary parts of QNMs frequencies are connected with the angular velocity and Lyapunov exponent of unstable circular null geodesics [61]. The perturbations by a scalar massless field around BHs are characterized by the effective potential barrier

$$V(r) = f(r)\left(\frac{f'(r)}{r} + \frac{l(l+1)}{r^2}\right), \tag{26}$$

where l being the multipole number $0, 1, 2....$ Equation (26) can be represented in the terms of dimensionless variable $x = r/\sqrt[4]{\beta q_m^2}$ as

$$V(x)\sqrt{\beta} q_m = f(x)\left(\frac{f'(x)}{x} + \frac{l(l+1)}{x^2}\right). \tag{27}$$

The effective potential is plotted in Figure 2 for $a = 5$, $b = 2$, $c = 1$ and $l = 1, 2, 3$ and for $a = 5$, $c = 1$, $l = 1$ and $b = 1, 2, 3$. According to Figure 2, Subplot l, shows that the effective potentials represent a potential barrier with a maximum. The height of the potential increases when the l increases. In accordance with Figure 2, Subplot 2, the height of the potential increases if the parameter b increases. The real and imaginary parts of quasinormal frequencies are given by [59,60]

$$\text{Re}\,\omega = \frac{l}{r_s} = \frac{l\sqrt{f(r_p)}}{r_p}, \quad \text{Im}\,\omega = -\frac{2n+1}{2\sqrt{2}r_s}\sqrt{2f(r_p) - r_p^2 f''(r_p)}, \tag{28}$$

where r_s is the BH shadow radius (the impact parameter), r_p is the radius of the BH photon sphere, $n = 0, 1, 2, ...$ is the overtone number. The real and imaginary parts of the frequencies versus the parameter b at $a = 5$, $c = 1$, $n = 1$, $l = 5$ are given in Table 2.

The imaginary parts of the frequencies in Table 2 are negative, and therefore, the modes are stable and the real part represents the frequency of oscillations. According to Table 2 when the parameter b increases the real part of the reduced frequency $\sqrt[4]{\beta q_m^2}\text{Re}\,\omega$ increases, but absolute value of the imaginary part of the reduced frequency $|\sqrt[4]{\beta q_m^2}\text{Im}\,\omega|$ decreases. In other words, increasing the parameter b the scalar perturbations oscillate with greater frequency and decay slowly. To study the dependence of frequencies on parameters α, β, M, q_m one has to put numerical numbers for these parameters in Equation (28).

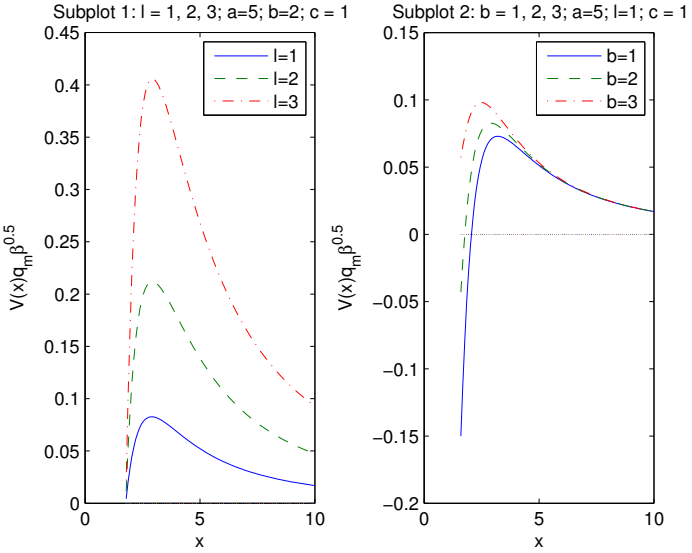

Figure 2. The plot of the function $V(x)\sqrt{\beta} q_m$ for $a = 5$, $c = 1$.

Table 2. The real and the imaginary parts of the frequencies vs the parameter b at $n = 1$, $l = 5$, $a = 5$, $c = 1$.

b	1.5	1.7	2	2.2	2.4	2.5	2.6
$\sqrt[4]{\beta q_m^2}\mathrm{Re}\ \omega$	0.865	0.877	0.899	0.914	0.931	0.940	0.951
$-\sqrt[4]{\beta q_m^2}\mathrm{Im}\ \omega$	0.2212	0.2208	0.2202	0.2191	0.2170	0.2163	0.2149

7. Deflection Angle

Let us study the light deflection angle by the BH solution (10). We can determine the total deflection angle $\Delta\varphi$ by the formula [62] (see also [63])

$$\Delta\varphi = 2\int_{r_p}^{\infty} \frac{dr}{r\sqrt{\frac{r^2 f(r_p)}{r_p^2} - f(r)}} - \pi, \tag{29}$$

where r_p is the photon sphere radius. Taking into account that $r_p/\sqrt{f(r_p)} = r_s$ is the shadow sphere radius ($r_s = \xi$ is the impact parameter) one can represent Equation (29) in terms of the dimensionless variable as

$$\Delta\varphi = 2\int_{x_p}^{\infty} \frac{dx}{x\sqrt{\frac{x^2}{x_s^2} - f(x)}} - \pi. \tag{30}$$

Making use of data in Table 1 we obtain the deflection angles from Equation (30) represented in Table 3.

Table 3. The deflection angles for a = 5, c = 1.

b	0.5	0.9	1.5	1.7	1.8	2	2.2	2.3	2.4	2.5	2.6
$\Delta\varphi$	4.12	3.58	3.1	3.02	2.96	2.86	2.81	2.77	2.76	2.73	2.69

According to Table 3 when the parameter b increasing, with fixed a and c, the deflection angle is decreased. One can also study the dependence of the deflection angle on parameters β, α, q_m and M by taking the numerical values for these parameters and putting them in Equation (10), finding the solution for r_p: $2f(r_p) - r_p f'(r_p) = 0$ ($r_s = r_p/\sqrt{f(r_p)}$), and calculating the integral (29).

8. Conclusions

We use the exact spherically symmetric and magnetically charged BH solution in 4D EGB gravity coupled to NED obtained in [36] for further investigations. It is shown that we have the Reissner–Nordström behavior of the charged BH at infinity. The logarithmic correction to the Bekenstein–Hawking entropy is obtained from first law of BH thermodynamics. Similar corrections to the area law are appeared in quantum gravity. We obtain the solution for the event horizon radius when the entropy becomes zero. For the light BHs the logarithmic correction is important while for massive BHs (for a big event horizon radius) such correction is small. Then, the energy emission rate of BHs has been studied. We showed that the BH energy emission rate decreases with increasing the model parameter b and the BH has a bigger lifetime. To verify that the energy density is positive as measured by any local observer and the sound speed does not exceed the light speed, we investigate the energy conditions. It has been demonstrated that WEC, DEC and SEC are satisfied. The quasinormal modes that describe small perturbations around BHs are investigated. We have been studied the dependence of the hight of the effective potential barrier on the multipole number l and model parameter b. The height of the potential increases when

the l or b increases. Complex frequencies, where the real part represents the frequency of oscillations and imaginary part characterises the oscillation decay, are calculated. We demonstrate that increasing the parameter b the scalar perturbations oscillate with greater frequency and decay slowly. Then, the gravitational lensing of light around BHs is studied by calculating the deflection angle $\Delta\varphi$ for some parameters. The deflection angle depends on the photon sphere radius r_p, shadow radius r_s and model parameters. It is shown that $\Delta\varphi$ is decreased if the parameter b increasing at fixed a and c.

Funding: This research received no external funding.

Institutional Review Board Statement: Not applicable.

Informed Consent Statement: Not applicable.

Data Availability Statement: Not applicable.

Conflicts of Interest: The author declares no conflict of interest.

References

1. Donoghue, J.F.; Menezeshttps, G. Unitarity, stability and loops of unstable ghosts. *Phys. Rev. D* **2019**, *100*, 105006. [CrossRef]
2. Platania, A.; Wetterich, C. Non-perturbative unitarity and fictitious ghosts in quantum gravity. *Phys. Lett. B* **2020**, *811*, 135911. [CrossRef]
3. Bojowald, M.; Paily, G.M.; Reyes, J.D. Discreteness corrections and higher spatial derivatives in effective canonical quantum gravity. *Phys. Rev. D* **2014**, *90*, 025025. [CrossRef]
4. Bojowald, M.; Ding, D. Canonical description of cosmological backreaction. *JCAP* **2021**, *3*, 083. [CrossRef]
5. Glavan, D.; Lin, C. Einstein-Gauss-Bonnet Gravity in Four-Dimensional Spacetime. *Phys. Rev. Lett.* **2020**, *124*, 081301. [CrossRef]
6. Fernandes, P.G.S. Charged black holes in AdS spaces in 4D Einstein Gauss-Bonnet gravity. *Phys. Lett. B* **2020**, *805*, 135468. [CrossRef]
7. Konoplya, R.A.; Zhidenko, A. Black holes in the four-dimensional Einstein-Lovelock gravity. *Phys. Rev. D* **2020**, *101*, 084038. [CrossRef]
8. Jusufi, K. Nonlinear magnetically charged black holes in 4D Einstein–Gauss–Bonnet gravity. *Ann. Phys.* **2020**, *421*, 168285. [CrossRef]
9. Ghosh, S.G.; Singh, D.V.; Kumar, R.; Maharaj, S.D. Phase transition of AdS black holes in 4D EGB gravity coupled to nonlinear electrodynamics. *Ann. Phys.* **2021**, *424*, 168347. [CrossRef]
10. Ghosh, S.G.; Maharaj, S.D. Radiating black holes in the novel 4D Einstein–Gauss–Bonnet gravity. *Phys. Dark Univ.* **2020**, *30*, 100687. [CrossRef]
11. Kumar, R.; Ghosh, S.G. Rotating black holes in 4D Einstein-Gauss-Bonnet gravity and its shadow. *JCAP* **2020**, *7*, 053 [CrossRef]
12. Jin, X.H.; Gao, Y.X.; Liu, D.J. Strong gravitational lensing of a 4-dimensional Einstein-Gauss-Bonnet black hole in homogeneous plasma. *Int. J. Mod. Phys. D* **2020**, *29*, 2050065. [CrossRef]
13. Jusufi, K.; Banerjee, A.; Ghosh, S.G. Wormholes in 4D Einstein–Gauss–Bonnet gravity. *Eur. Phys. J. C* **2020**, *80*, 698. [CrossRef]
14. Guo, M.; Li, P. Innermost stable circular orbit and shadow of the 4D Einstein–Gauss–Bonnet black hole. *Eur. Phys. J. C* **2020**, *80*, 588. [CrossRef]
15. Zhang, C.; Zhang, S.; Li, P.; Guo, M. Superradiance and stability of the regularized 4D charged Einstein-Gauss-Bonnet black hole. *JHEP* **2020**, *8*, 105. [CrossRef]
16. Zhang, C.; Li, P.; Guo, M. Greybody factor and power spectra of the Hawking radiation in the 4D Einstein–Gauss–Bonnet de-Sitter gravity. *Eur. Phys. J. C* **2020**, *80*, 874. [CrossRef]
17. Odintsov, S.; Oikonomou, V.; Fronimos, F. Rectifying Einstein-Gauss-Bonnet inflation in view of GW170817. *Nucl. Phys. B* **2020**, *958*, 115135. [CrossRef]
18. Ai, W. A note on the novel 4D Einstein–Gauss–Bonnet gravity. *Commun. Theor. Phys.* **2020**, *72*, 095402. [CrossRef]
19. Fernandes, P.G.; Carrilho, P.; Clifton, T.; Mulryne, D.J. Derivation of regularized field equations for the Einstein-Gauss-Bonnet theory in four dimensions. *Phys. Rev. D* **2020**, *102*, 024025. [CrossRef]
20. Panah, B.E.; Jafarzade, K.; Hendi, S.H. Charged 4D Einstein-Gauss-Bonnet-AdS black holes: Shadow, energy emission, deflection angle and heat engine. *Nucl. Phys. B* **2020**, *961*, 115269. [CrossRef]
21. Hennigar, R.A.; Kubiznak, D.; Mann, R.B.; Pollack, C. On taking the D $\rightarrow$ 4 limit of Gauss-Bonnet gravity: Theory and solutions. *JHEP* **2020**, *2020*, 27. [CrossRef]
22. Cai, R.G.; Cao, L.M.; Ohta, N. Black holes in gravity with conformal anomaly and logarithmic term in black hole entropy. *JHEP* **2010**, *1004*, 082. [CrossRef]
23. Cai, R.-G. Thermodynamics of conformal anomaly corrected black holes in AdS space. *Phys. Lett. B* **2014**, *733*, 183. [CrossRef]
24. Gurses, M.; Sisman, T.C.; Tekin, B. Comment on "Einstein-Gauss-Bonnet Gravity in Four-Dimensional Spacetime". *Phys. Rev. Lett.* **2020**, *125*, 149001. [CrossRef] [PubMed]

25. Gurses, M.; Sisman, T.C.; Tekin, B. Is there a novel Einstein–Gauss–Bonnet theory in four dimensions? *Eur. Phys. J. C* **2020**, *80*, 647. [CrossRef]
26. Mahapatra, S. A note on the total action of 4D Gauss–Bonnet theory. *Eur. Phys. J. C* **2020**, *80*, 992. [CrossRef]
27. Kobayashi, T. Effective scalar-tensor description of regularized Lovelock gravity in four dimensions. *JCAP* **2020**, *7*, 013. [CrossRef]
28. Bonifacio, J.; Hinterbichler, K.; Johnson, L.A. Amplitudes and 4D Gauss-Bonnet theory. *Phys. Rev. D* **2020**, *102*, 024029. [CrossRef]
29. Arrechea, J.; Delhom, A.; Jiménez-Cano, A. Inconsistencies in four-dimensional Einstein-Gauss-Bonnet gravity. *Chin. Phys. C* **2021**, *45*, 013107. [CrossRef]
30. Hohmann, M.; Pfeifer, C.; Voicu, N. Canonical variational completion and 4D Gauss–Bonnet gravity. *Eur. Phys. J. Plus* **2021**, *136*, 180. [CrossRef]
31. Aoki, K.; Gorji, M.A.; Mukohyama, S. A consistent theory of D– 4 Einstein-Gauss-Bonnet gravity. *Phys. Lett. B* **2020**, *810*, 135843. [CrossRef]
32. Aoki, K.; Gorji, M.A.; Mukohyama, S. Cosmology and gravitational waves in consistent D– 4 Einstein-Gauss-Bonnet gravity. *JCAP* **2020**, *2009*, 014. [CrossRef]
33. Aoki, K.; Gorji, M.A.; Mizuno, S.; Mukohyama, S. Inflationary gravitational waves in consistent D– 4 Einstein-Gauss-Bonnet gravity. *JCAP* **2021**, *2101*, 054. [CrossRef]
34. Jafarzade, K.E.; Zangeneh, M.K.; Lobo, F.S.N. Shadow, deflection angle and quasinormal modes of Born-Infeld charged black holes. *JCAP* **2021**, *4*, 008. [CrossRef]
35. Kruglov, S.I. Nonlinear Electrodynamics and Magnetic Black Holes. *Ann. Phys. (Berlin)* **2017**, *529*, 1700073. [CrossRef]
36. Kruglov, S.I. 4D Einstein–Gauss–Bonnet Gravity Coupled with Nonlinear Electrodynamics. *Symmetry* **2021**, *13*, 204. [CrossRef]
37. Yang, K.; Gu, B.M.; Wei, S.W.; Liu, Y.X. Born–Infeld black holes in 4D Einstein–Gauss–Bonnet gravity. *Eur. Phys. J. C* **2020**, *80*, 662. [CrossRef]
38. Kumar, A.; Kumar, R.; Bardeen black holes in the novel 4D Einstein–Gauss–Bonnet gravity. *arXiv* **2003**, arXiv:2003.13104.
39. Kumar, A.; Ghosh, S.G.; Hayward black holes in the novel 4D Einstein–Gauss–Bonnet gravity. *arXiv* **2004**, arXiv:2004.01131.
40. Ghosh, S.G.; Singh, D.V.; Maharaj, S.D. Regular black holes in Einstein-Gauss-Bonnet gravity. *Phys. Rev. D* **2018**, *97*, 104050. [CrossRef]
41. Konoplya, R.A.; Zinhailo, A.F. Quasinormal modes, stability and shadows of a black hole in the 4D Einstein-Gauss-Bonnet gravity. *Eur. Phys. J. C* **2020**, *80*, 1049. [CrossRef]
42. Konoplya, R.A.; Zinhailo, A.F. 4D Einstein-Lovelock black holes: Hierarchy of orders in curvature. *Phys. Lett. B* **2020**, *807*, 135607. [CrossRef]
43. Belhaj, A.; Benali, M.; Balali, A.E.; Moumni, H.E.; Ennadifi, S.E. Deflection angle and shadow behaviors of quintessential black holes in arbitrary dimensions. *Class. Quant. Grav.* **2020**, *37*, 215004. [CrossRef]
44. Konoplya, R.A.; Stuchlik, Z. Are eikonal quasinormal modes linked to the unstable circular null geodesics? *Phys. Lett. B* **2017**, *771*, 597. [CrossRef]
45. Stefanov, I.Z.; Yazadjiev, S.S.; Gyulchev, G.G. Connection between black-hole quasinormal modes and lensing in the strong deflection limit. *Phys. Rev. Lett.* **2010**, *104*, 251103. [CrossRef]
46. Guo, Y.; Miao, Y.G. Null geodesics, quasinormal modes and the correspondence with shadows in high-dimensional Einstein-Yang-Mills spacetimes. *Phys. Rev. D* **2020**, *102*, 084057. [CrossRef]
47. Wei, S.W.; Liu, Y.X. Null geodesics, quasinormal modes, and thermodynamic phase transition for charged black holes in asymptotically flat and dS spacetimes. *Chin. Phys. C* **2020**, *44*, 115103. [CrossRef]
48. Bronnikov, K.A. Regular magnetic black holes and monopoles from nonlinear electrodynamics. *Phys. Rev. D* **2001**, *63*, 044005. [CrossRef]
49. Boulware, D.G.; Deser, S. String-Generated Gravity Models. *Phys. Rev. Lett.* **1985**, *55*, 2656. [CrossRef]
50. Medved, A.J.M.; Vagenas, E.C. When conceptual worlds collide: The generalized uncertainty principle and the Bekenstein-Hawking entropy. *Phys. Rev. D* **2004**, *70*, 124021. [CrossRef]
51. Cognola, G.; Myrzakulov, R.; Sebastiani, L.; Zerbini, S. Einstein gravity with Gauss-Bonnet entropic corrections. *Phys. Rev. D* **2013**, *88*, 024006. [CrossRef]
52. Cvetic, M.; Nojiri, S.; Odintsov, S.D. Black hole thermodynamics and negative entropy in de Sitter and anti-de Sitter Einstein–Gauss–Bonnet gravity. *Nucl. Phys. B* **2002**, *628*, 295. [CrossRef]
53. Mashhoon, B. Scattering of Electromagnetic Radiation from a Black Hole. *Phys. Rev. D* **1973**, *7*, 2807. [CrossRef]
54. Misner, C.W.; Thorne, K.S.; Wheeler, J.A. *Gravitation*; W.H. Freeman and Company: San Francisco, CA, USA, 1973.
55. Decanini, Y.; Esposito-Farese, G.; Folacci, A. Universality of high-energy absorption cross sections for black holes. *Phys. Rev. D* **2011**, *83*, 044032. [CrossRef]
56. Wei, S.W.; Liu, Y.X. Observing the shadow of Einstein-Maxwell-Dilaton-Axion black hole. *JCAP* **2013**, *11*, 063. [CrossRef]
57. Dymnikova, I. Regular electrically charged vacuum structures with de Sitter centre in nonlinear electrodynamics coupled to general relativity. *Class. Quant. Grav.* **2004**, *21*, 4417. [CrossRef]
58. Hawking, S.W.; Ellis, G.F.R.; *The Large Scale Structure of Space-Time*; Canbridge Univ. Press: Canbridge, UK, 1973.
59. Jusufi, K. Quasinormal modes of black holes surrounded by dark matter and their connection with the shadow radius. *Phys. Rev. D* **2020**, *101*, 084055. [CrossRef]

60. Jusufi, K. Connection Between the Shadow Radius and Quasinormal Modes in Rotating Spacetimes. *Phys. Rev. D* **2020**, *101*, 124063. [CrossRef]
61. Cardoso, V.; Miranda, A.S.; Berti, E.; Witek, H.; Zanchin, V.T. Geodesic stability, Lyapunov exponents, andquasinormal modes. *Phys. Rev. D* **2009**, *79*, 064016. [CrossRef]
62. Weinberg, S. *Gravitation and Cosmology: Principles and Applications of the General Theory of Relativity*; Wiley: New York, NY, USA, 1972.
63. Kocherlakota, P.; Rezzolla, L. Accurate mapping of spherically symmetric black holes in a parameterised framework. *Phys. Rev. D* **2020**, *102*, 064058. [CrossRef]